doi:10.1017/S1431927622002355
Microsc. Microanal. 28 (Suppl 1), 2022

Segmentation of "Important" Features in in High Dimensional Nanodiffraction Datasets

Carter Francis[1], Paul Voyles[1*]

[1.] Department of Materials Science and Engineering, University of Wisconsin-Madison, Madison, Wi, US.
* Corresponding author: paul.voyles@wisc.edu

Recent advances in electron microscopy, including small convergent electron beams (nm to Angstroms in diameter) and ultrafast detectors capable of acquiring 1,000-100,000 frames per second have given rise to a broad class of experiments under the moniker "4-D STEM". In these experiments, a small probe is rastered over a sample and a nanodiffraction pattern $I(k_x, k_y)$ is measured at each real space position (x, y) in the material. Local structure in the material is probed at (x, y) with each nanodiffraction pattern containing important information about the structure at that position.

Techniques for analysis of 4D STEM data are almost always automated due to the size and complexity of the datasets. Tens to hundreds of GB datasets are commonplace and ultrafast detectors routinely acquire TB sized datasets. Methods for automated analysis include image filtering-based techniques such as symmetry STEM [2,3], angular correlations [1], and fluctuation microscopy [4]. Other methods identify specific diffraction features using peak finding methods for extraction of diffraction vectors at each (x, y) [5,6]. These methods can provide detailed analysis but are sensitive to the number of electrons and may miss many less intense diffraction features.

We have developed a general methodology for finding a set of "important" diffraction features in a high dimensional data like 4D STEM datasets. This method is well-suited to data sets with low signal measured from complex samples. We define important features as features with significant extent in both (k_x, k_y) and (x, y). The size can be adjusted, but the minimum size should be the diameter of the beam in real space and the convergence angle in reciprocal space. This requirement increases robustness against noise and reduces the chances of mis-identifying features from dynamic/inelastic scattering or other sources.

The method is a generalization of the Laplacian of Gaussian approach [7] with specific parameters for 4-D STEM data. It can be described as follows for a 4-D dataset: (1) Apply a 4-D Gaussian filter to the data with a kernel $(\sigma_{\boldsymbol{r}}, \sigma_{\boldsymbol{k}}) = (r_{beam(\boldsymbol{r})} * \sqrt{2}, r_{beam(\boldsymbol{k})} * \sqrt{2})$ where $r_{beam(r/k)}$ is the radius of the beam in (x, y) and the convergence angle in (k_x, k_y) respectively and $(\sigma_{\boldsymbol{r}}, \sigma_{\boldsymbol{k}})$ is sigma for the gaussian kernel in (x, y) and (k_x, k_y) respectively; (2) Calculate the Laplacian of the filtered data; (3) Identify local minima in the data from (2) as important features; (4) Refine and combine features from (3). The Gaussian filter acts like a bandpass filter, reducing contributions from features in the dataset which are less than the size of the beam and the convergence angle and therefore unphysical. It also smooths the data, reducing noise. The Laplacian is the second derivate in n dimensions, so peaks in the original data are local minima in the Laplacian. These local minima represent the set of "important" 4-D vectors in the data. Further processing determines their spatial extent in (x,y) and clusters them in (x,y) to create diffraction patterns arising from the same spatial object. The set of important 4-D vectors captures the information content in the original data at dramatically reduced data size. The method has been implemented in the pyxem package [8] and operates using out of memory operations using multiple cores.

Figure 1 shows analysis of a 4D STEM dataset acquired from a polycrystalline Al thin film on a carbon support with multiple overlapping grains. Figure 1a is the annular dark field STEM image. Figure 1b is a false colored image recreated from only the crystals identified from the important diffraction features. Overlapping grains in different orientations are readily distinguished. Figure 1c shows diffraction patterns recreated from two grains close to [011] and [111] zone axes. Automated analysis of similar reconstructed patterns could be used for orientation imaging on background-free, denoised data.

Figure 2 shows similar analysis applied to a PdCuSi metallic glass. Speckle patterns from metallic glasses contain many "unimportant" speckles arising from random overlaps of atoms through the thickness of the sample, combined with dynamical and inelastic scattering. Figure 2a is a virtual darkfield image recreated from only the important diffraction features. This image emphasizes regions of the glass with strong structural order. Figure 2b-e show example reconstructed diffraction patterns with strong but partially complete 2-,4-,6- and 10-fold symmetries.

The Authors acknowledge funding and considerations from the following sources. [9]

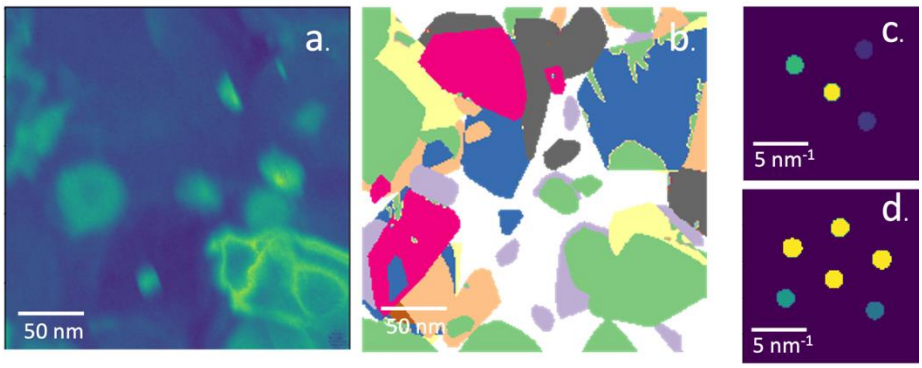

Figure 1: Analysis of 4D STEM data from a polycrystalline thin film. (a) annular darkfield image (b) all the nanocrystals identified, including overlapping crystals and crystals with weak diffraction that are not visible in (a). (c) and (d) reconstructed diffraction patterns from crystals close to [011] and [111] zone axes, respectively.

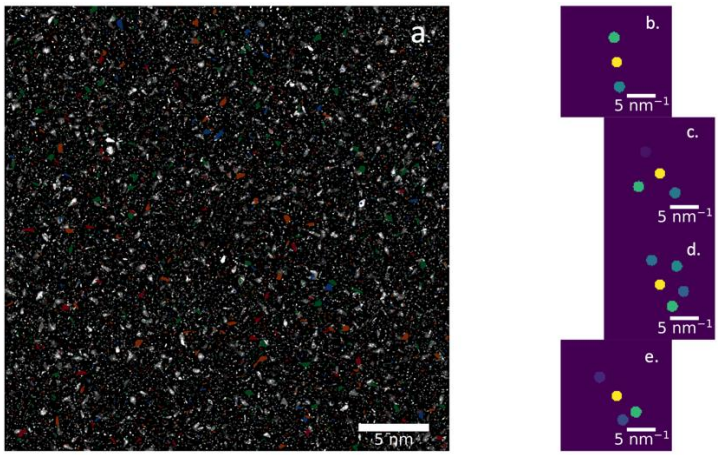

Figure 2: Analysis of 4D STEM data from a PdCuSi metallic glass thin film. (a) virtual darkfield image created from only the important diffraction features. High symmetry clusters are colored blue for 2-fold

https://doi.org/10.1017/S1431927622002355 Published online by Cambridge University Press

symmetry, orange for 4-fold, red for 6-fold, and green for 10-fold. (b) – (e) example reconstructed diffraction patterns with at least partial versions of each symmetry.

References:

[1] Im, S. et al., *Ultramicroscopy* ***195*** (2018), p. 189–193.

[2] Krajnak, M. and Etheridge, J. *Proceedings of the National Academy of Sciences of the United States of America* **117** (2020), p. 27805–27810

[3] Huang S. et al. *Ultramicroscopy* ***232*** *(2022) 113405*

[4] P.M. Voyles and D.A. Muller, *Ultramicroscopy* ***93*** (2002), p. 147–159.

[5] Johnstone, D. N. et al. *Journal of Applied Crystallography.* **53** *(*2020), p**.**1293–1298.

[6] Savitzky, B. H., et al. *Microscopy and Microanalysis*, ***27*** (2021) p.712–743.

[7] Kong, H., Akakin, H. C., & Sarma, S. E. *IEEE Transactions on Cybernetics*, ***43*****(6)**, (2013) p. 1719–1733.

[8] *pyXEM*. (n.d.). https://doi.org/10.5281/zenado.2649351

[9] This research was supported by the Wisconsin Materials Research Science and Engineering Center (DMR-1720415).